DOI: 10.15199/17.2022.5.1

Natural gas hydrates in flow assurance

Hydraty gazu ziemnego w zapewnieniu przepływu

Ferdinand Uilhoorn *)

Keywords: *Hydrates; Pipeline blockage; Transient gas flow*

Abstract
This work focuses on hydrate formation in natural gas pipelines, which is considered as the principal flow assurance problem. A hydrate phase equilibrium model is combined with a transient gas flow model to monitor if, where, and when natural gas in pipelines enters the hydrate formation region. The hydrate model is based on phase equilibria in systems with natural gas containing free and dissolved water. A transient gas flow model is used to describe the flow conditions in natural gas pipelines. This approach enables pipeline operators to monitor the risk of hydrates under normal and emergency conditions, but also to estimate the optimal trade-off between different hydrate prevention techniques. To show the applicability of the method a case study is conducted for a subsea pipeline.

Słowa kluczowe: *Hydraty; Zatykanie rurociągów; Nieustalony przepływ gazu*

Streszczenie
W niniejszej pracy skupiono się na tworzeniu się hydratów w rurociągach gazu ziemnego, co jest uważane za główny problem związany z zapewnieniem przepływu. Model równowagi fazowej hydratów jest połączony z modelem nieustalonego przepływu gazu w celu monitorowania, czy, gdzie i kiedy gaz ziemny w rurociągach wchodzi w obszar tworzenia się hydratów. Model hydratów opiera się na równowagach fazowych w systemach, w których gaz ziemny zawiera wolną i rozpuszczoną wodę. Do opisu warunków przepływu w rurociągach gazu ziemnego wykorzystywany jest model przepływu gazu w warunkach nieustalonych. Takie podejście umożliwia operatorom rurociągów monitorowanie ryzyka powstawania hydratów w warunkach normalnych i awaryjnych, a także oszacowanie optymalnego kompromisu między różnymi technikami zapobiegania powstawaniu hydratów. Aby pokazać możliwość zastosowania metody, przeprowadzono studium przypadku dla rurociągu podmorski.

1. Introduction

Natural gas hydrates are ice-like solid compounds of small gas molecules and water. These compounds form when molecules such as methane, ethane, propane, carbon-dioxide, or hydrogen sulphide are in contact with water at low temperature and high pressure. The gas molecules are encaged by cavities, which are hydrogen bonded and stabilized by van der Waals forces. Figure 1 illustrates a methane molecule that is trapped by water molecules.

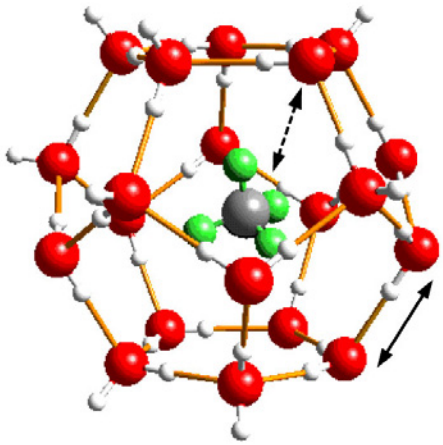

Fig. 1. A methane hydrate. Hydrogen bonding (↔) and Van der Waals type of interaction (⇠⇢).

Rys. 1. Hydrat metanu. Wiązanie wodorowe (↔) i oddziaływanie typu Van der Waalsa (⇠⇢).

Gas hydrates can be classified in three different structures, i.e., I, II and H depending on the cavities and their size (see Table 1 and Figure 2). The properties of hydrates give rise to different fields. First, massive dissociation of methane hydrates on the ocean floor could increase the amount of greenhouse gases in the atmosphere. This threat is related to the "clathrate gun hypothesis" which suggests that variations in sea level pressure and temperature during glacial cycles caused episodes of methane hydrate dissociation, strengthening global climate changes [2]. Second, methane hydrates have the potential to contain 164 m^3 gas m^{-3} of hydrate [3]. This property makes them attractive for transport and storage [4–5].

Table 1. Lattice properties of structure I, II and H [1].

Tabela 1. Właściwości struktury I, II i H [1].

	sI		sII		sH		
Description	5^{12}	$5^{12}6^2$	5^{12}	$5^{12}6^4$	5^{12}	$4^35^66^3$	$5^{12}6^8$
Average cell radius, *Rm* (Å) [a]	3.95	4.30	3.91	4.73	≈ 3.91 [b]	≈ 4.06 [b]	≈ 5.71 [b]
Coordination number, *z* [c]	20	24	20	28	20	20	36
Water molecules per unit cell	46		136		34		
Cavities per unit cell	2	6	16	8	3	2	1
Crystal type	Cubic		Cubic		Hexagonal		

[a] The average cavity radius includes the radius of the water molecules in the cavity wall.
[b] Based on geometric models.
[c] Number of oxygen molecules at the periphery of each cavity.

*) **Ferdinand Uilhoorn** – Department of Heating and Gas Systems, Warsaw University of Technology, Nowowiejska 20, 00-653 Warsaw, ferdinand.uilhoorn@pw.edu.pl.

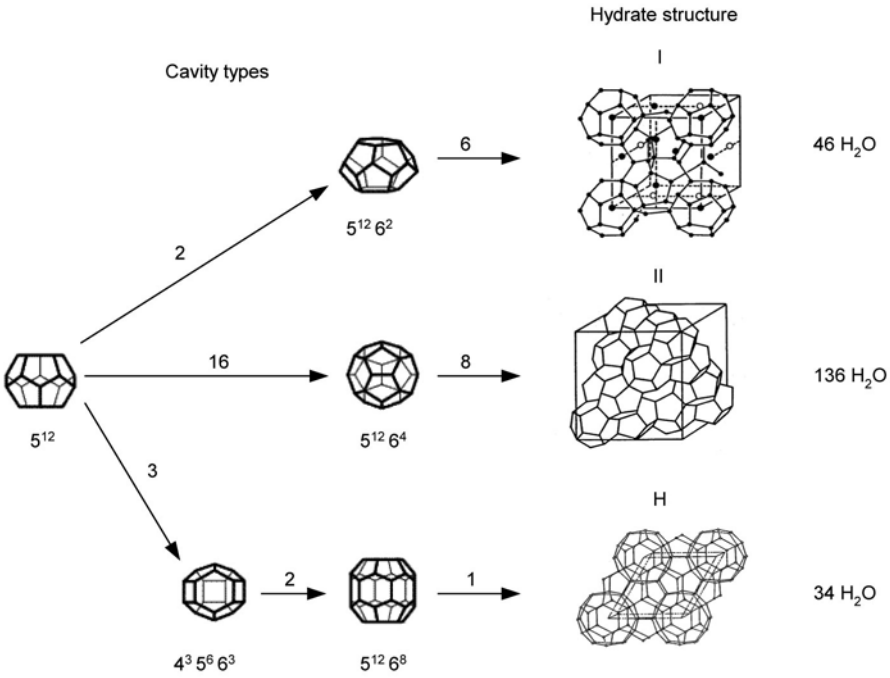

Fig. 2. The three common hydrate unit crystal structures. Here, 51264 means a water cage with 12 pentagonal and four hexagonal faces. The numbers refer to the number of cage types. For example, for structure I, we have a unit crystal with two 512 cages, six 51262 cages and 46 water molecules [1].

Rys. 2. Trzy powszechnie występujące struktury krystaliczne jednostek hydratów. Tu 51264 oznacza klatkę wodną o 12 ścianach pięciokątnych i czterech sześciokątnych. Liczby odnoszą się do liczby typów klatek. Na przykład, w strukturze I mamy jednostkę krystaliczną z dwiema klatkami 512, sześcioma klatkami 51262 i 46 cząsteczkami wody [1].

Third, a large fraction of the Earth's fossil fuel is stored in hydrates. During the last years, the estimates decreased from 20,000 tcm to 3000 tcm [6–8]. Nevertheless, if we compared these estimates with the conventional gas resources (□404 tcm) and shale gas (204–456 tcm) it is still enormous [9]. Fourth, hydrates are of risk in oil and gas pipeline because under thermodynamically favourable conditions, such as the deep-sea conditions they agglomerate, create plugs and may finally block pipelines, heat exchangers and compressors causing costly production stops (see Figure 3). Prevention techniques are focused on water removal, chemical injection (thermodynamic, kinetic and/or anti-agglomerants), depressurization, thermal heating, and/or improving pipeline insulation. It should be mentioned that the requisite that free water (i.e., aqueous phase) must be present in pipelines to form hydrates is a common misunderstanding. From a thermodynamic perspective, hydrocarbon in the vapor or liquid phase with dissolved water can still form hydrates [11]. The aim of this work is to combine transient gas flow modelling with hydrate phase equilibrium modelling for monitoring the hydrate risk. This is important during normal exploitation, but especially in case of emergency situations such as pipeline leakage [12] or failure of dehydration systems [13].

Fig. 3. Gas hydrate plug in a subsea pipeline [10].

Rys. 3. Zator hydratu gazowego w rurociągu podmorskim [10].

The prediction of hydrate kinetics is a challenging problem because the difficulty lies here in the stochastic nature of the formation process [14]. However, by considering the classical thermodynamics as the boundary of hydrate kinetics and having information about the flow transients in pipeline systems we are able to estimate the hydrate risk and to define the cost-optimal hydrate prevention parameters.

In this work, the natural gas is treated as a single-phase flow, where it is assumed that the small amount of free water has a negligible effect on the flow conditions. Therefore, the proposed method is limited to systems containing small amounts of free water and dried gas, that may appear in, for example onshore and offshore pipelines, but also export lines leaving the process platform to the coast. Flowlines from the subsea well to a manifold or directly from the well to the platforms carry most often a mixture of gas, oil, condensate, and water and require a multiphase flow model. This is beyond the scope of this work, but an important direction for future works.

The rest of this work is organized as follows. In Section 2, we introduce the hydrate equilibrium model. The transient gas flow model is briefly discussed in Section 3. A case-study for a real pipeline configuration is presented in Section 4 while concluding remarks are included in Section 5.

2.Hydrate equilibirum model

The hydrate equilibrium model is based on statistical mechanics derived by Van der Waals and Platteeuw [15]. This model is based on the following assumptions: (i) no distortion of the host lattice by the caged molecules, (ii) only one molecule is encaged and no diffusion takes place, (iii) no interactions exist between the solute molecules, and (iv) classical statistics are valid where quantum effects are ignored.

As a result of these assumptions, the chemical potential of water (w) in the hydrate (H) relative to a hypothetical empty lattice (β) can be described as

$$\Delta\mu_w^{(\beta-H)} = \mu_w^{(\beta)} - \mu_w^{(H)} = -RT\sum_m \nu_m \ln\left(1-\sum_k y_{k,m}\right), \quad (1)$$

where V_m is the number of cages of type m in the unit cell, T is the temperature, R is the gas constant, and $V_{k,m}$ is the fractional occupancy of guest species k in hydrate cages of type m. The chemical potential between the hydrate phase and the coexisting water phase (liquid L or ice α), must be equal,

$$\Delta\mu_w^{(\beta-H)} = \mu_w^{\beta} - \mu_w^{H} = \mu_w^{\beta} - \mu_w^{L\ or\ \alpha} = \Delta\mu_w^{(\beta-L\ or\ \alpha)}. \quad (2)$$

In terms of fugacity we can write, $f_w^{(H)} = f_w^{(L\ or\ \alpha)}$ where the fugacity of water in the hydrate phase is defined as

$$f_w^{(H)} = f_w^{(\beta)} e^{\left(\sum_m \nu_m \ln\left(1-\sum_k y_{k,m}\right)\right)}. \quad (3)$$

The fractional occupancy is obtained as follows

$$y_{k,m} = \frac{C_{k,m} f_k}{1 + \sum_{i=1} C_{i,m} f_i}, \tag{4}$$

where $C_{k,m}$ is the Langmuir constant and f_k is the gas fugacity. The Langmuir constant represents the gas-water interactions in the cavity and is given by

$$C_{k,m} = \frac{4\pi}{kT} \int_0^R \exp\left(-\frac{\omega(r)}{kT} \right) r^2 dr, \tag{5}$$

where R is the cell radius of the cavity. The spherical cell potential $\omega(r)$ is defined as [16]

$$\omega(r) = 2z\varepsilon \left[\frac{\sigma^{12}}{R^{11} r} \left(\delta^{10} + \frac{a}{R} \delta^{11} \right) - \frac{\sigma^6}{R^5 r} \left(\delta^4 + \frac{a}{R} \delta^5 \right) \right], \tag{6}$$

with

$$\delta^N = \frac{1}{N} \left[\left(1 - \frac{r}{R} - \frac{a}{R} \right)^{-N} - \left(1 + \frac{r}{R} - \frac{a}{R} \right)^{-N} \right], \tag{7}$$

where z is the coordination number of the cavity and N is 4, 5, 10 or 11. The Kihara parameters are denoted as σ, ε and a and fitted from experimental data.

The chemical potential of liquid water is formulated as

$$f_w^{(L)} = f_w^{(\beta)} \exp\left(\left[\frac{\mu_w^{(\beta,0)} - \mu_w^{(L,0)}}{RT_0} \right] - \int_{T_0}^{T} \left[\frac{H^{(\beta)} - H^{(L)}}{RT^2} \right] dT + \int_{P_0}^{P} \left[\frac{V^{(\beta)} - V^{(L)}}{RT} \right] dp - \ln\left(x_w \gamma_w \right) \right), \tag{8}$$

and for pure ice

$$f_w^{(\alpha)} = f_w^{(\beta)} \exp\left(\left[\frac{\mu_w^{(\beta,0)} - \mu_w^{(\alpha,0)}}{RT_0} \right] - \int_{T_0}^{T} \left[\frac{H^{(\beta)} - H^{(\alpha)}}{RT^2} \right] dT + \int_{P_0}^{P} \left[\frac{V^{(\beta)} - V^{(\alpha)}}{RT} \right] dp \right), \tag{9}$$

with superscript 0 as the reference state, enthalpy H and molar volume V of ice, liquid water and empty hydrate, activity coefficient γ_w and mole fraction of water in aqueous phase x_w. The latter is obtained from

$$x_w = 1 - \sum_{i=1}^{n} x_{i,w}. \tag{10}$$

The activity coefficient is calculated from the UNIFAC model [17] and the composition of the guest molecule in the liquid phase $x_{i,w}$ is obtained from Henry's law, $x_{i,w} = f_{i,g}/H_{i,w}$. Here $f_{i,g}$ is the fugacity of the gas component i and x_i is the mole fraction of the gas dissolved in water. The effect of pressure on Henry's constant $H_{i,w}$ is described by the Krichevsky-Kasarnovsky equation [18].

Now by equating $f_w^{(H)} = f_w^{(L \text{ or } \alpha)}$ the hydrate formation conditions can be calculated. To determine the phase of the mixture a multiphase flash calculation is conducted. The predictive Soave-Redlich-Kwong (PSRK) group contribution method [19] is used to calculate the fugacity of all components in vapor and liquid phases. The computation procedure assumes that we have free water in the system. In case of two-phase equilibria, the algorithm is slightly modified, whereas the hydrate pressure or temperature is calculated by equating, $f_w^{(H)} = f_{w,g}^{L}$, where $f_{w,g}^{L}$ is the fugacity of water in the hydrocarbon calculated with the PSRK method. The fugacity of the empty hydrate, $f_w^{(\beta)}$ is obtained from the correlation

$$\ln\left(f_w^{(\beta)} \right) = \sum_{i=0}^{a_n} a_i p^{I_{i,0}} T^{I_{i,1}}, \tag{11}$$

where I denotes the power term and a are coefficients.

3.Transient gas flow model

The transient flow model constitutes a nonhomogeneous system of partial differential equations derived from the conservation principles of mass, momentum, and energy. The set of equations reads [20]

$$\frac{\partial p}{\partial t} = \frac{a_s^2}{c_p T} \left(1 + \frac{T}{z} \left(\frac{\partial z}{\partial T} \right)_p \right) \left(\frac{q}{A} + \frac{\dot{m} z R T}{p A^2} w \right) - \left[\frac{\dot{m} z R T}{pA} - \frac{a_s^2 \dot{m}}{pA} \left(1 - \frac{p}{z} \left(\frac{\partial z}{\partial p} \right)_T \right) \right] \frac{\partial p}{\partial x} - \frac{a_s^2 \dot{m}}{TA} \left(1 + \frac{T}{z} \left(\frac{\partial z}{\partial T} \right)_p \right) \frac{\partial T}{\partial x} - \frac{a_s^2}{A} \frac{\partial \dot{m}}{\partial x}, \tag{12}$$

$$\frac{\partial T}{\partial t} = \frac{a_s^2}{c_p p} \left(1 - \frac{p}{z} \left(\frac{\partial z}{\partial p} \right)_T \right) \left(\frac{q}{A} + w \frac{\dot{m} z R T}{p A^2} \right) - \frac{\dot{m} z R T}{pA} \frac{\partial T}{\partial x} - \frac{a_s^2}{c_p} \left(1 + \frac{T}{z} \left(\frac{\partial z}{\partial T} \right)_p \right) \times \left[\frac{\dot{m} z R}{pA} \left(1 + \frac{T}{z} \left(\frac{\partial z}{\partial T} \right)_p \right) \frac{\partial T}{\partial x} - \frac{\dot{m} T R z}{p^2 A} \left(1 - \frac{p}{z} \left(\frac{\partial z}{\partial p} \right)_T \right) \frac{\partial p}{\partial x} + \frac{z T R}{pA} \frac{\partial \dot{m}}{\partial x} \right], \tag{13}$$

$$\frac{\partial \dot{m}}{\partial t} = -\frac{\dot{m}}{T} \left(1 + \frac{T}{z} \left(\frac{\partial z}{\partial T} \right)_p \right) \frac{\partial T}{\partial t} + \frac{\dot{m}}{p} \left(1 - \frac{p}{z} \left(\frac{\partial z}{\partial p} \right)_T \right) \frac{\partial p}{\partial t} - \frac{\dot{m}^2 z R}{pA} \left(1 + \frac{T}{z} \left(\frac{\partial z}{\partial T} \right)_p \right) \frac{\partial T}{\partial x} + \left(\frac{\dot{m}^2 T R z}{p^2 A} \left(1 - \frac{p}{z} \left(\frac{\partial z}{\partial p} \right)_T \right) - A \right) \frac{\partial p}{\partial x} - \frac{\dot{m} z T R}{pA} \frac{\partial \dot{m}}{\partial x} - w - \frac{pAg \sin(\theta)}{zTR}, \tag{14}$$

where pressure p, mass flow rate $\dot{m}$, temperature T, cross-sectional area A, frictional force w, gravitational acceleration g, angle of inclination θ, heat flow q, compressibility factor z, frictional force per unit length w, specific heat at constant pressure c_p, and isentropic wave speed a_s. The heat transfer between the fluid and the soil per unit length and time is defined as

$$q = -\pi d U \left(T - T_s \right), \tag{15}$$

where U is the total heat transfer coefficient and T_s is the surrounding temperature. The compressibility factor is calculated by the PSRK method.

The partial differential equations (12)-(14) are spatially discretized and converted into a system of ordinary differential equations. A five-point, fourth-order finite difference scheme is used for the spatial discretization. The system of ordinary differential equations is solved with a second-order accurate implicit Runge-Kutta algorithm.

4.Case study

In this section, a case study is conducted using the pipeline parameters of the Baltic project [21], in particular, the offshore part of the Baltic seabed.[1)] The 275 km pipeline has a diameter of 900 mm. The molar fraction of the gas is: 98.3455 CH_4, 0.6104 C_2H_6, 0.1572 C_3H_8, 0.0299 i-C_4H_{10}, 0.0253 n-C_4H_{10}, 0.0055 i-C_5H_{12}, 0.0040 n-C_5H_{12}, 0.0303 N_2 and 0.7918 CO_2. Simulations are performed assuming an overall heat transfer of 1.0 W/m^{2}K and 2.0 W/m^{2}K, which corresponds to dry and wet insulation, respectively [22]. The seabed temperature is assumed to be 4 °C. The boundary conditions are $p(0,t) = 10.5$ MPa, $T(0,t) = 40$ °C, $\dot{m}(L, t) = f(t)$ with function $f(t)$ shown in Figure 3.

1) Only the pipeline dimensions of the Baltic project are used here because information about gas composition, boundary conditions or insulation properties are unknown and therefore selected arbitrarily.

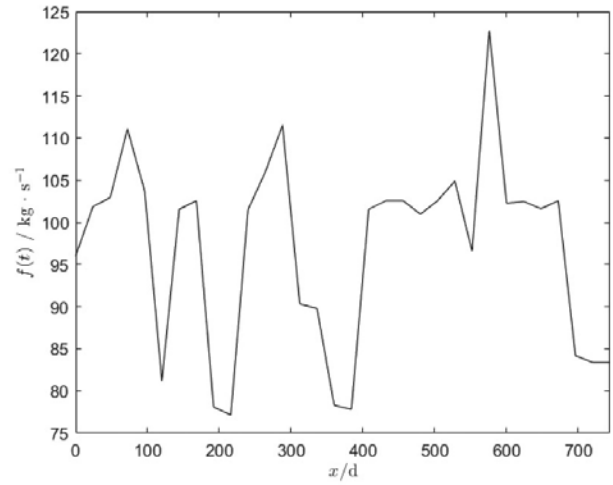

Fig. 3. Boundary conditions at the pipeline outlet.
Rys. 3. Warunki brzegowe na wylocie rurociągu.

85.5 ppm still imposes the risk of hydrates. This is also illustrated in Figure 5 where the time and location of the gas entering the hydrate region for both water contents are calculated. For the natural gas with a water content of 85.5 ppm, a discontinuous line is observed. In this situation, the gas remains mainly outside the hydrate formation region, but not all the time. This means that, depending on the cost, the water content of the gas should be further decreased and/or better insulation properties should be applied. The pressure and temperature trajectory, including time and location of intersection with the hydrate locus (151 ppm) are shown in Figures 6 and 7, respectively.

A similar analysis can be conducted for other prevention techniques such as line heaters or thermodynamic inhibitors. It should be mentioned that the results are valid within the assumptions and approximations made. For example, other gas compositions and/or boundary conditions will give different results. Besides that, we focused on hydrate prevention, other important issues within flow assurance such as corrosion mitigation might decide differently.

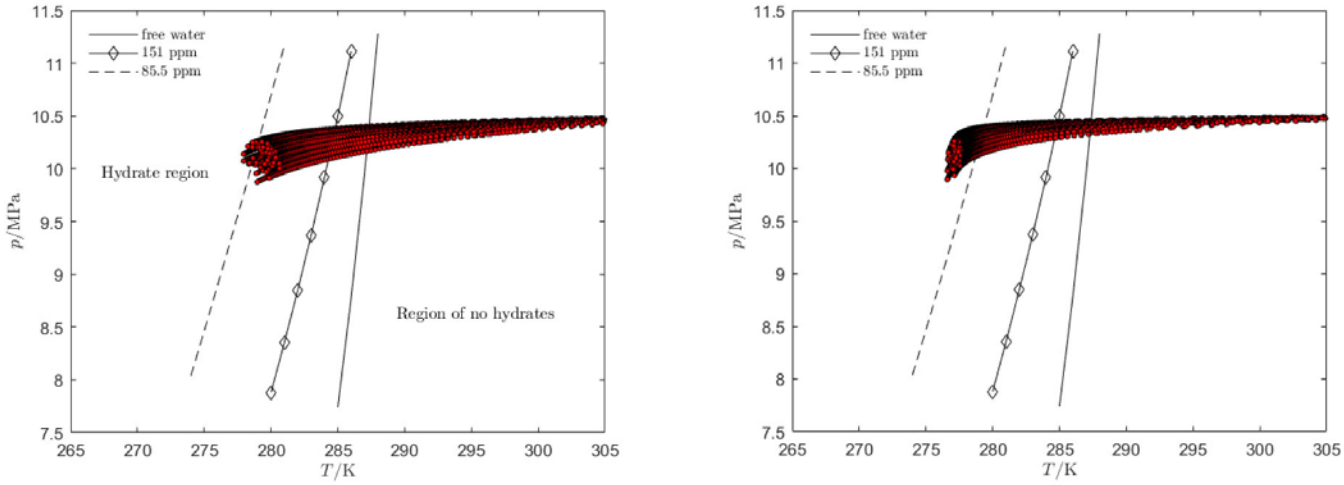

Fig. 4. Hydrate loci for saturated and dried natural gas and p,T conditions in the pipeline. U = 1.0 W/m2K (left) and U = 2.0 W/m2K (right).
Rys. 4. Krzywe hydratów dla gazu ziemnego nasyconego i suchego oraz warunków p,T w rurociągu. U = 1.0 W/m2K (po lewej) i U = 2.0 W/m2K (po prawej).

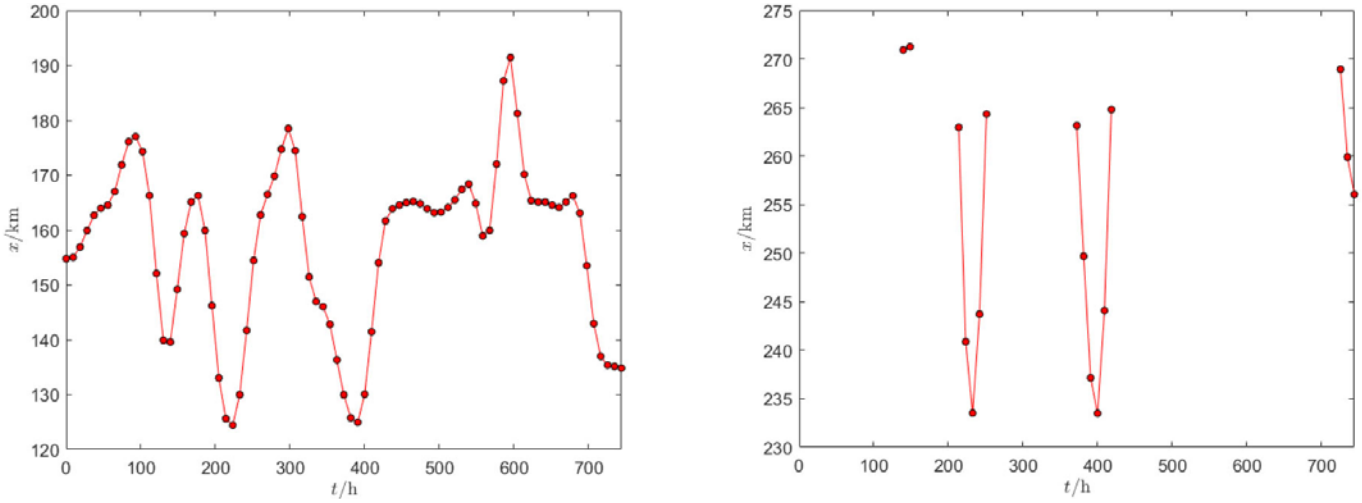

Fig. 5. Time and location when the natural gas enters the hydrate formation region. Dry gas with a water content of 151 ppm (left) and 85.5 ppm (right). U = 1.0 W/m2K.
Rys. 5. Czas i miejsce wejścia gazu ziemnego w obszar tworzenia się hydratów. Suchy gaz o zawartości wody 151 ppm (po lewej) i 85.5 ppm (po prawej). U = 1.0 W/m2K.

A typical water content after the process of dehydration lies between 85.5 ppm and 151 ppm [23]. The corresponding hydrate loci, together with the pipeline pressure and temperature values, both in time and space are shown in Figure 4. The latter values are computed with the transient flow model (12)-(14). The results infer that even improving the insulation (U = 1.0 W/m^{2}K) a moisture content of

5.Conclusion

In this work, hydrate and transient gas flow modeling were coupled. This approach enables pipeline operators to monitor the risk of possible hydrate formation and to determine the time and location at which the natural gas enters the hydrate formation region. The case-study for the offshore pipeline showed that a water content of 85.5

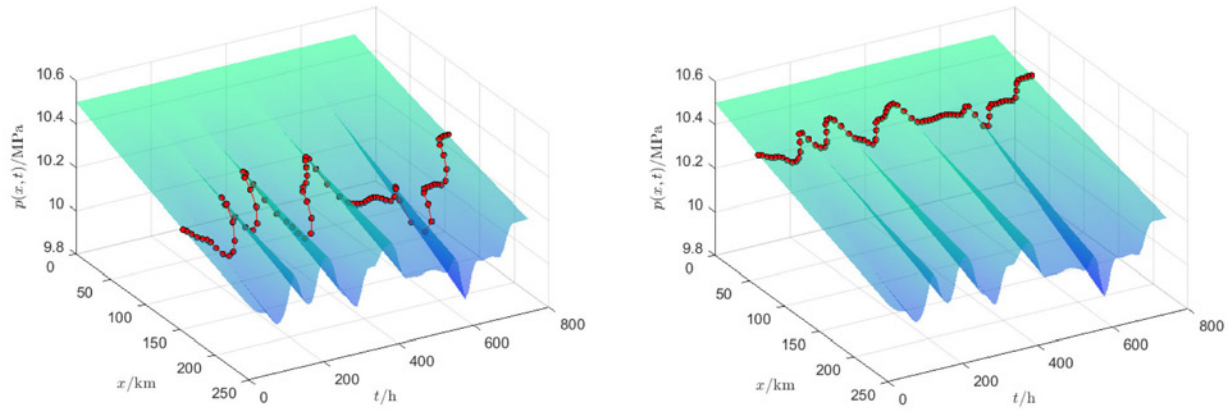

Fig. 6. Pressure trajectory and intersection with the hydrate locus for natural gas dried to 151 ppm. U = 1.0 W/m²K (left) and U = 2.0 W/m²K (right).

Rys. 6. Przebieg ciśnienia i przecięcie z krzywą hydratu dla gazu ziemnego osuszonego do poziomu 151 ppm. U = 1.0 W/m²K (po lewej) i U = 2.0 W/m²K (po prawej).

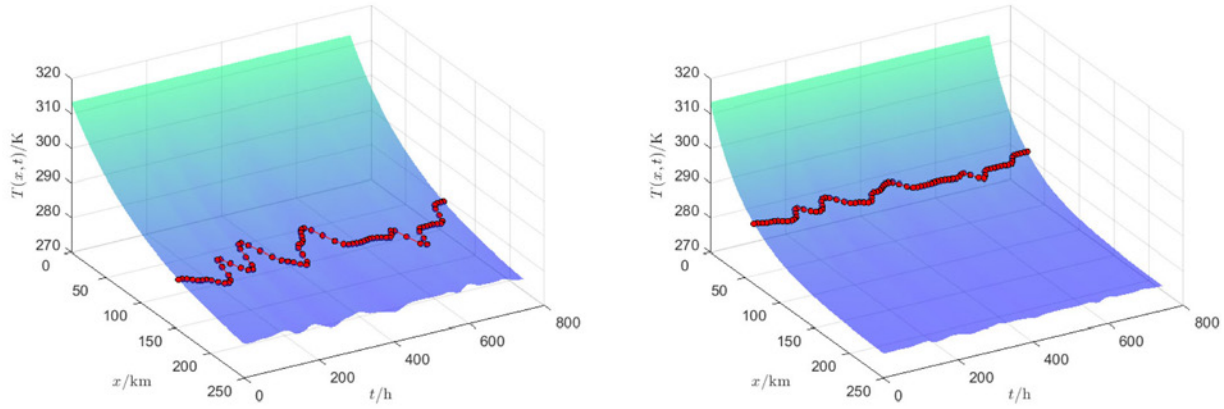

Fig. 7. Temperature trajectory and intersection with the hydrate locus for natural gas dried to 151 ppm. U = 1.0 W/m²K (left) and U = 2.0 W/m²K (right).

Rys. 7. Przebieg temperatury i przecięcie z krzywą hydratu dla gazu ziemnego osuszonego do poziomu 151 ppm. U = 1.0 W/m²K (po lewej) i U = 2.0 W/m²K (po prawej).

ppm is not sufficient to exclude hydrate risk. The proposed method not only enables pipeline operators to estimate if there is a risk of hydrates, but also to find the optimal trade-off between different hydrate prevention techniques.

Although, this work considers natural gas pipelines, the proposed method can be extended to pipeline carrying carbon-dioxide in gas, liquid, dense or supercritical phase. For future work, it is advocated to consider multiphase flow model where flowlines from the subsea well to a manifold or platforms can be considered. ■

REFERENCES

[1] E. D. Sloan Jr, 2003. "Fundamental principles and applications of natural gas hydrates," *Nature*, 426, 6964, 353–363.

[2] J. P. Kennett, K. G. Cannariato, I. L. Hendy, and r. J. Behl. 2002. "Methane hydrates in Quaternary climate change: The clathrate gun hypothesis." Washington, DC: Am Geophys Union.

[3] I. Chatti, A. Delahaye, L. Fournaison, and J.-P. Petitet. 2005. "Benefits and drawbacks of clathrate hydrates: a review of their areas of interest." *Energy Convers. Manage*., 46, 9, 1333–1343.

[4] S. Thomas and r. A. Dawe. 2003. "Review of ways to transport natural gas energy from countries which do not need the gas for domestic use." 28, 14, 1461-1477.

[5] J. S. Gudmundsson and A. Børrehaug. 1996. "Frozen hydrate for transport of nature gas." in *2nd International Conference on Nature Gas Hydrate*, Toulouse, France.

[6] K. A. Kvenvolden. 1999. "Potential effects of gas hydrate on human welfare," *PNAS*, 96, 7, 3420–3426.

[7] A. V. Milkov. 2004. "Global estimates of hydrate-bound gas in marine sediments: how much is really out there?," *Earth-Sci*. Rev., 66, 3, 183–197.

[8] R. Boswell and T. S. Collett. 2011. "Current perspectives on gas hydrate resources." *Energy Environ*. Sci., 4, 4, 1206–1215.

[9] Z. r. Chong, S. H. B. Yang, P. Babu, P. Linga, and X.-S. Li 2016. "Review of natural gas hydrates as an energy resource: Prospects and challenges," *Appl. Energy*, 162, 1633–1652.

[10] "Why are gas hydrates important? – centre for gas hydrate research." [Online]. Available: https://hydrate.site.hw.ac.uk/why-are-gas-hydrates-important/. [Accessed: 04-May-2022].

[11] E. Dendy Sloan and Jr. 1998. *Clathrate Hydrates of Natural Gases*, Second Edition, Revised and Expanded. CRC Press.

[12] S. Zhai, C. Chauvet, r. Azarinezhad, and J. Zeng. 2015. "Discussion of pipeline leakage and hydrate formation risks associated in deepwater natural gas pipelines,"*17th International Conference on Multiphase Production Technology*, Cannes, France.

[13] J. D. Sundramoorthy, M. J. Leknes, and K. Moodley. 2018 "Unconventional Gas Dehydration System Failure Resulting in a Gas Hydrate Blockage," *Offshore Technology Conference*, Asia, Kuala Lumpur, Malaysia.

[14] C. A. Koh, E. D. Sloan, A. K. Sum, and D. T. Wu, "Fundamentals and applications of gas hydrates," *Annu. Rev. Chem. Biomol*. Eng., vol. 2, pp. 237–257, 2011.

[15] J. H. van der Waals, J. H. van der Waals, and J. C. Platteeuw, "Clathrate Solutions," *Advances in Chemical Physics*. pp. 1–57, 1959.

[16] V. McKoy and O. Sinanoğlu. 1963. "Theory of dissociation pressures of some gas hydrates," *J. Chem. Phys*., 38, 12, 2946–2956.

[17] A. Fredenslund, r. L. Jones, and J. M. Prausnitz. 1975 "Group-contribution estimation of activity coefficients in nonideal liquid mixtures," *AIChE J*., 21, 6, 1086–1099.

[18] I. r. Krichevsky and J. S. Kasarnovsky. 1935. "Thermodynamical Calculations of Solubilities of Nitrogen and Hydrogen in Water at High Pressures," *J. Am. Chem. Soc*., 57, 11, 2168–2171.

[19] T. Holderbaum and J. Gmehling. 1991. "PSRK: A group contribution equation of state based on UNIFAC," *Fluid Phase Equilib*., 70, 2–3, 251–265.

[20] F. E. Uilhoorn. 2017. "Comparison of Bayesian estimation methods for modeling flow transients in gas pipelines." *Journal of Natural Gas Science and Engineering*, 38, 159–170.

[21] https://www.baltic-pipe.eu/. [Accessed: 06-May-2022].

[22] N. Sunday, A. Settar, K. Chetehouna, and N. Gascoin 2021. "An overview of flow assurance heat management systems in subsea flowlines." *Energies*, 14, 2, 458.

[23] J. Carroll. 2014. "Dehydration of Natural Gas." *Natural Gas Hydrates*. 175–195.